Toward an Optimal Design of Deep Profiling Float Network

Shuhei MASUDA, Satoshi Osafune, Nozomi Sugiura,
Shigeki Hosoda, Taiyo Kobayashi, and Toshio Suga

Research and Development Center for Global Change,
Japan Agency for Marine-Earth Science and Technology (JAMSTEC), Yokosuka, Japan

Import role of Deep Ocean in global change (in an aspect of the earth energy budget)

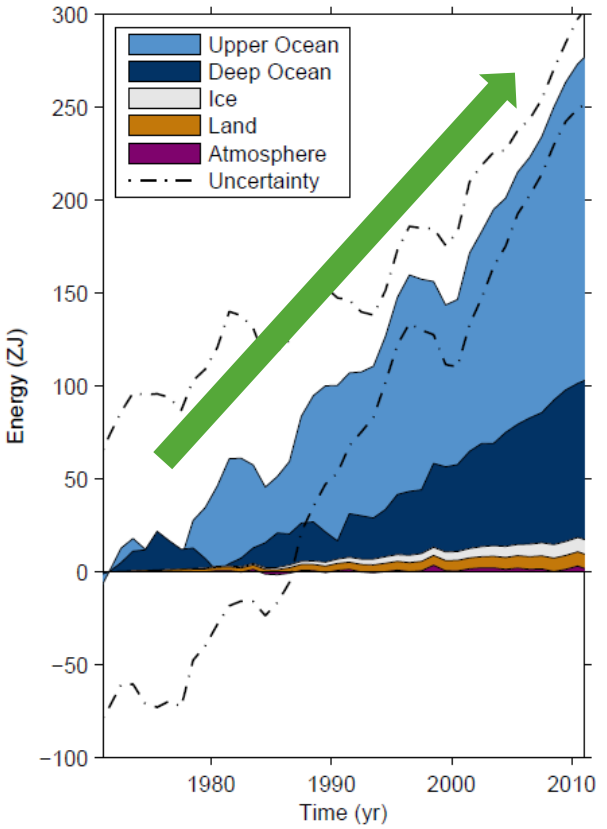

Increasing energy accumulati

Upper ocean heating (above 700m)

Deep ocean heating (below 700m)

Ice melt

Continental warming

Atmospheric warming

Box 3.1, Figure 1: Plot of energy accumulation in ZJ (1 ZJ = 10^{21} J) within distinct components of Earth's climate system relative to 1971 and from 1971–2010 unless otherwise indicated. See text for data sources. Ocean warming (heat content change) dominates, with the upper ocean (light blue, above 700 m) contributing more than the deep ocean (dark blue, below 700 m; including below 2000 m estimates starting from 1992). Ice melt (light grey; for glaciers and ice caps, Greenland and Antarctic ice sheet estimates starting from 1992, and Arctic sea ice estimate from 1979–2008); continental (land) warming (orange); and atmospheric warming (purple; estimate starting from 1979) make smaller contributions. Uncertainty in the ocean estimate also dominates the total uncertainty (dot-dashed lines about the error from all five components at 90% confidence intervals).

http://www.ipcc.ch/(IPCC 5th assessment report)

Vertical heat redistribution and climate change

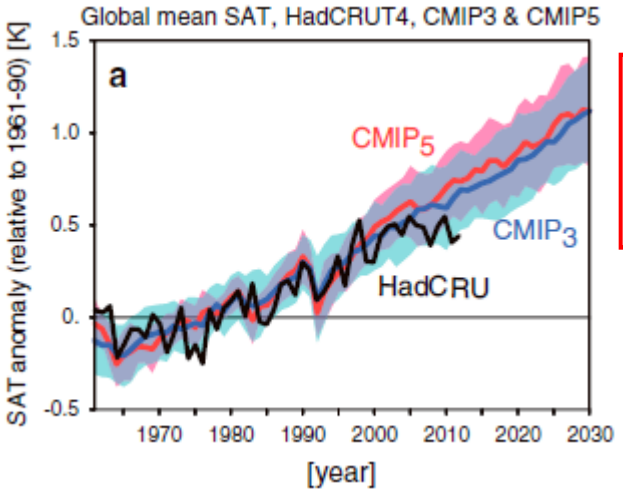

Strengthening of ocean heat uptake efficiency associated with the recent climate hiatus (GRL2013)

Masahiro Watanabe,[1] Youichi Kamae,[2] Masakazu Yoshimori,[1] Akira Oka,[1] Makiko Sato,[3,4] Masayoshi Ishii,[5] Takashi Mochizuki,[6] and Masahide Kimoto[1]

Figure 1. SAT_g anomalies relative to 1961–1990 means in observations and CMIP models. (a) Observed record (black curve) taken from HadCRUT4 and the simulations based on the ensemble averages of 20th century historical experiments of CMIP3 (blue) and CMIP5 (red) models. The standard deviation (σ) of the ensemble average is denoted by shading. The model values after 2000 and 2006 for CMIP3 and CMIP5 are from the A1b and RCP4.5 emission scenario runs, respectively. (b) 10 year mean SAT anom-

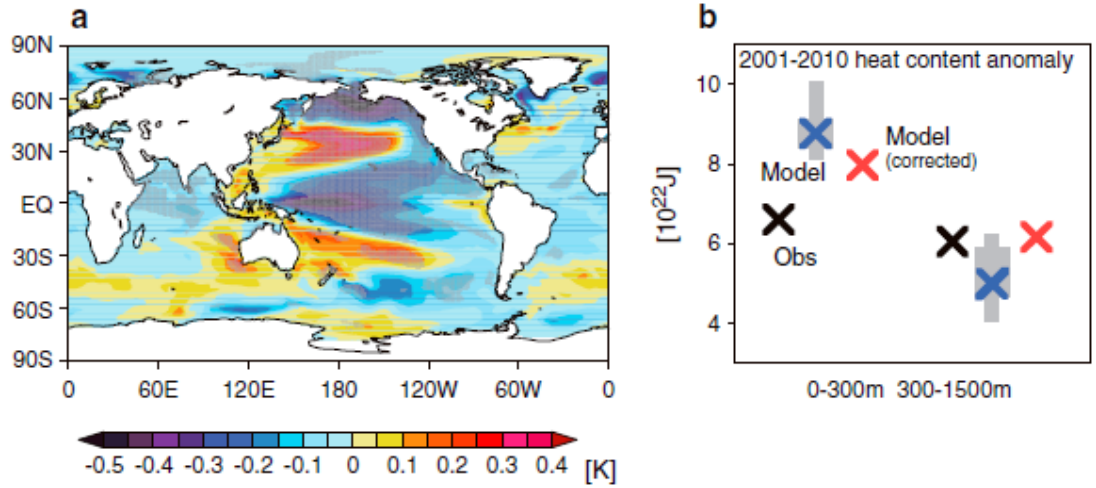

Figure 3. Natural ocean heat uptake variability and correction to simulated decadal-mean anomalies for 2001–2010. (a) Linear regression of the decadal-means of SST anomalies on the SAT_g anomaly among 11-member ensemble historical and RCP4.5 experiments by MIROC5. The ensemble means have been subtracted and the values indicate the SST anomaly per -1σ of SAT_g anomaly. Regressed anomalies significant at the 95% level are stippled. (b) Global-mean HC_{300} and HC_{1500} anomalies for 2001–2010, including observational data [*Ishii and Kimoto*, 2009] (black), ensemble mean of the MIROC5 simulation (blue), and the corrected ensemble mean (red). Thick and thin gray bars indicate 50% and 75% ranges of the ensemble, respectively.

Observations of deep ocean

Purkey and Johnson (2010)

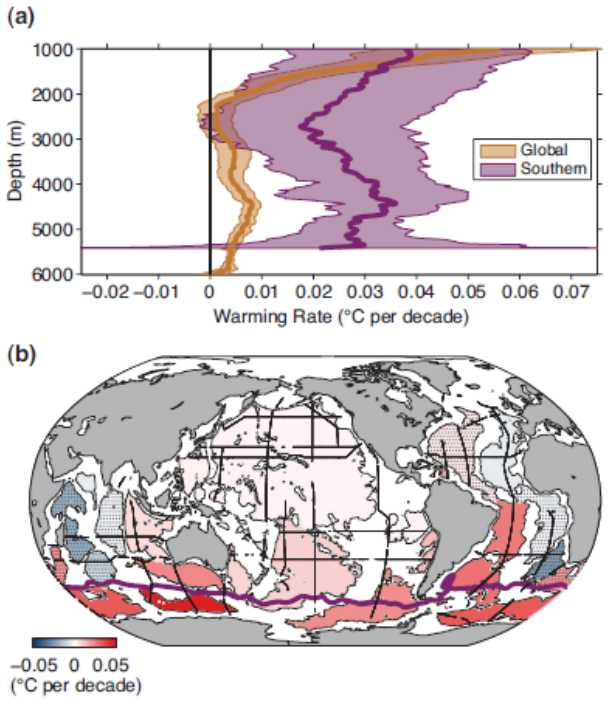

Figure 3.3: a) Areal mean warming rates (°C per decade) versus depth (thick lines) with 5 to 95% confidence limits (shading), both global (orange) and south of the Sub-Antarctic Front (purple), centred on 1992–2005. b) Mean warming rates (°C per decade) below 4000 m (colorbar) estimated for deep ocean basins (thin black outlines), centred on 1992–2005. Stippled basin warming rates are not significantly different from zero at 95% confidence. The positions of the Sub-Antarctic Front (purple line) and the repeat oceanographic transects from which these warming rates are estimated (thick black lines) also shown. Data from Purkey and Johnson (2010).

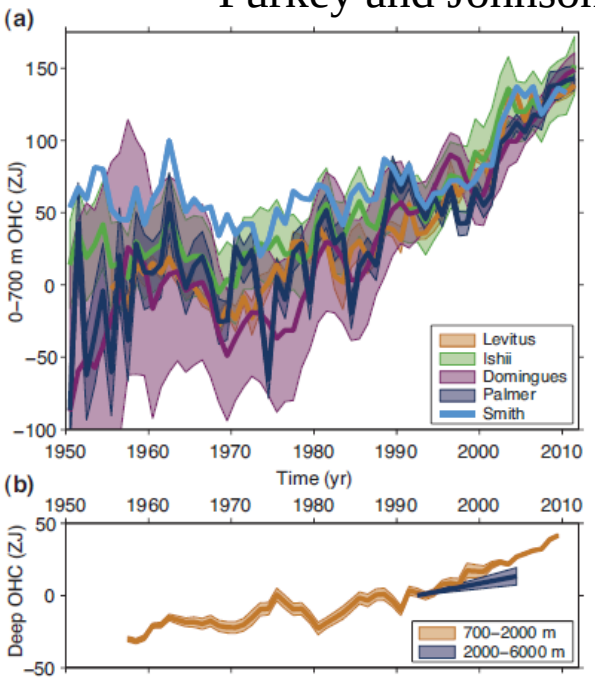

Figure 3.2: a) Observation-based estimates of annual global mean upper (0–700 m) ocean heat content in ZJ (1 ZJ = 10^{21} Joules) updated from (see legend): (Levitus et al., 2012), (Ishii and Kimoto, 2009), (Domingues et al., 2008), (Palmer et al., 2007), and (Smith and Murphy, 2007). Uncertainties are shaded, and plotted as published (at the one standard error level, except one standard deviation for Levitus, with no uncertainties provided for Smith). Estimates are shifted to align for 2006–2010, five years that are well measured by Argo, and then plotted relative to the resulting mean of all curves for 1971, the starting year for trend calculations. b) Observation-based estimates of annual five-year running mean global mean mid-depth (700–2000 m) ocean heat content in ZJ (Levitus et al., 2012) and the deep (2000 - 6000 m) global ocean heat content trend from 1992–2005 (Purkey and Johnson, 2010), both with one standard error uncertainties shaded (see legend).

Bottom-water warming

http://www.ipcc.ch/(IPCC 5th assessment repor

We have to know more about deep ocean

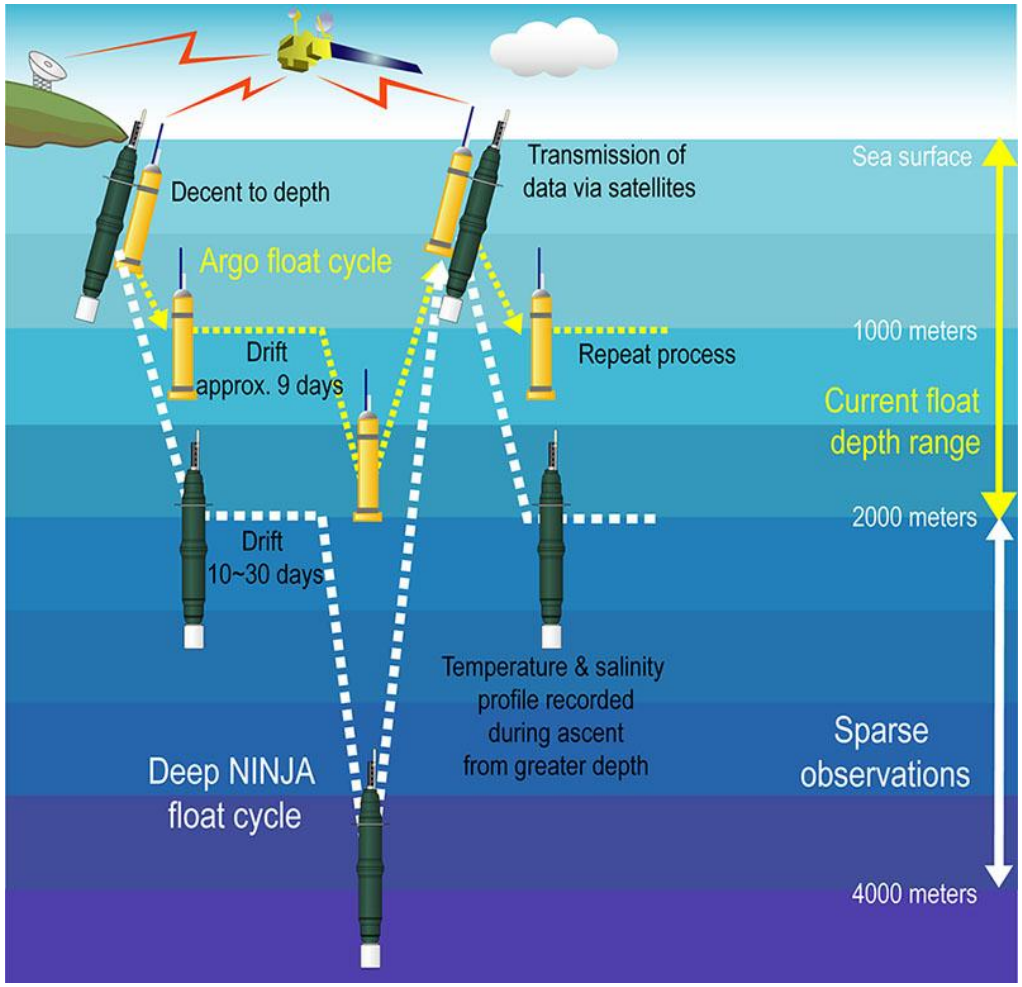

Deep Ninja developed by JAMSTEC/Tsurumi-Seiki

Designs for the next phase of Argo

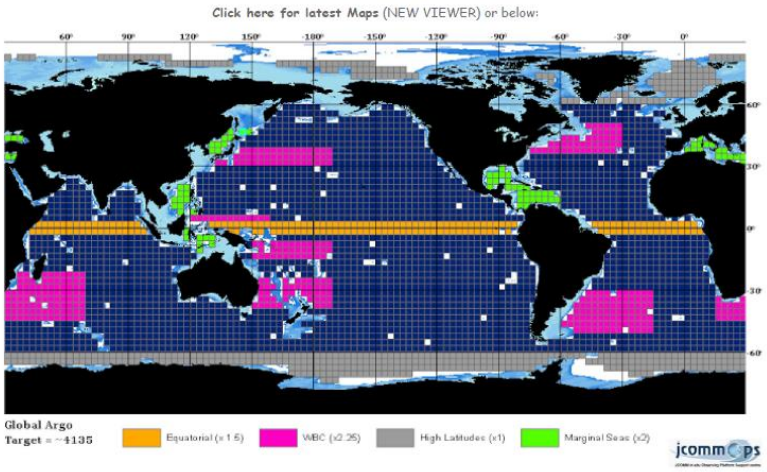

Revised Global Argo

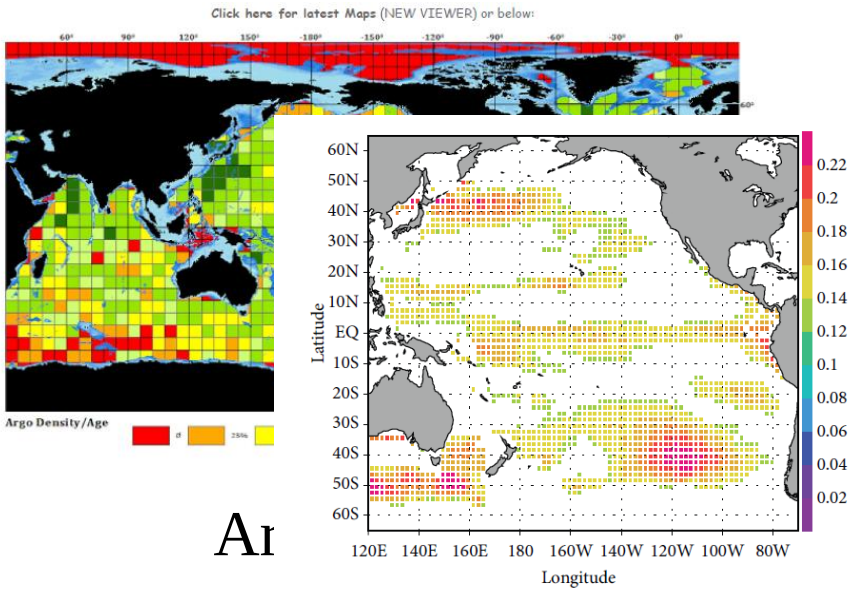

Ar

FIGURE 5: The same as Figure 4(b) but for the 1652 highest sensitivity values (see Section 3.2 in the text for details).

An optimal design for a specific climate change… (Masuda and Hosoda, 2014)

Designs of deep float network…..?

Optimal Observations for Variational Data Assimilation

ARMIN KÖHL AND DETLEF STAMMER

536 JOURNAL OF PHYSICAL OCEANOGRAPHY VOLUME 34

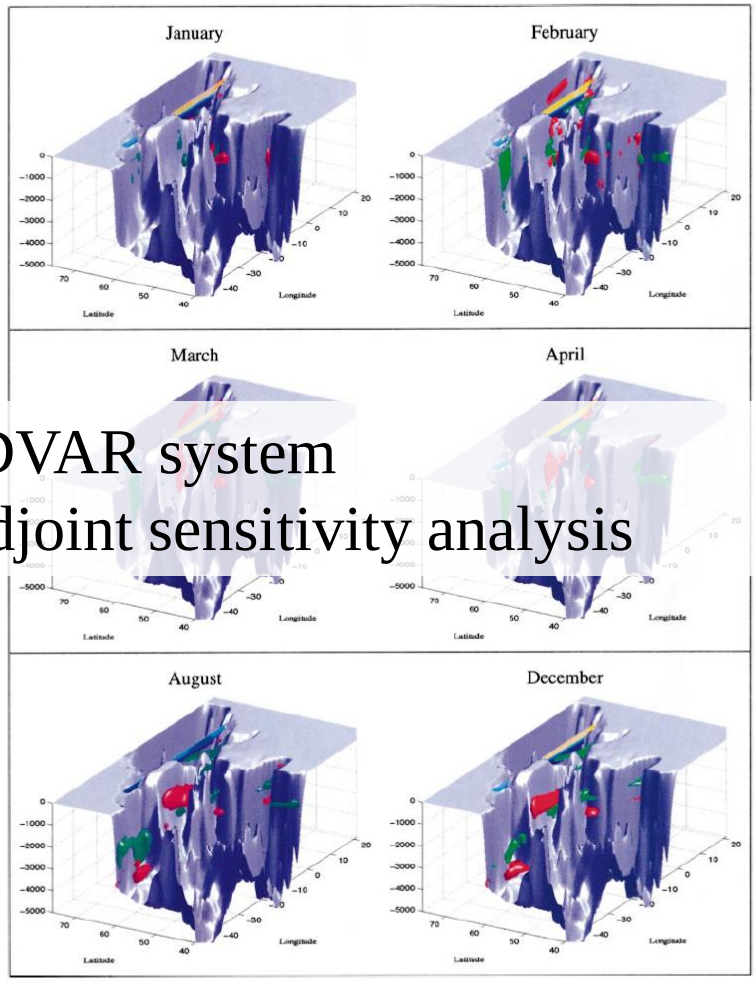

FIG. 5. Location of hydrographic observations that are optimal for inferring Feb meridional heat transport across the GSR. Red and green surfaces are isosurfaces (positive and negative, respectively) of the gradient of the heat transport with respect to temperature observations for the illustrated months. The gradient was multiplied with the square root of temperature error weight. The threshold for the isosurfaces is at ±3.5 TW. Regions without optimal observations, i.e., without any noticeable impact on the cost function, are not shown in the figure. The section is marked in yellow and blue. The threshold value for the gradient $\partial h/\partial y$ was adjusted in order to have the same number of hydrographic data at optimal locations as the number of data sampled in a monthly section. The total number of data points in the 12 months is 7764 for temperature.

- 4DVAR system
- Adjoint sensitivity analysis

JPO2004

Optimal observations for mass transport through a strait was carefully proposed.

Adjoint sensitivity analysis

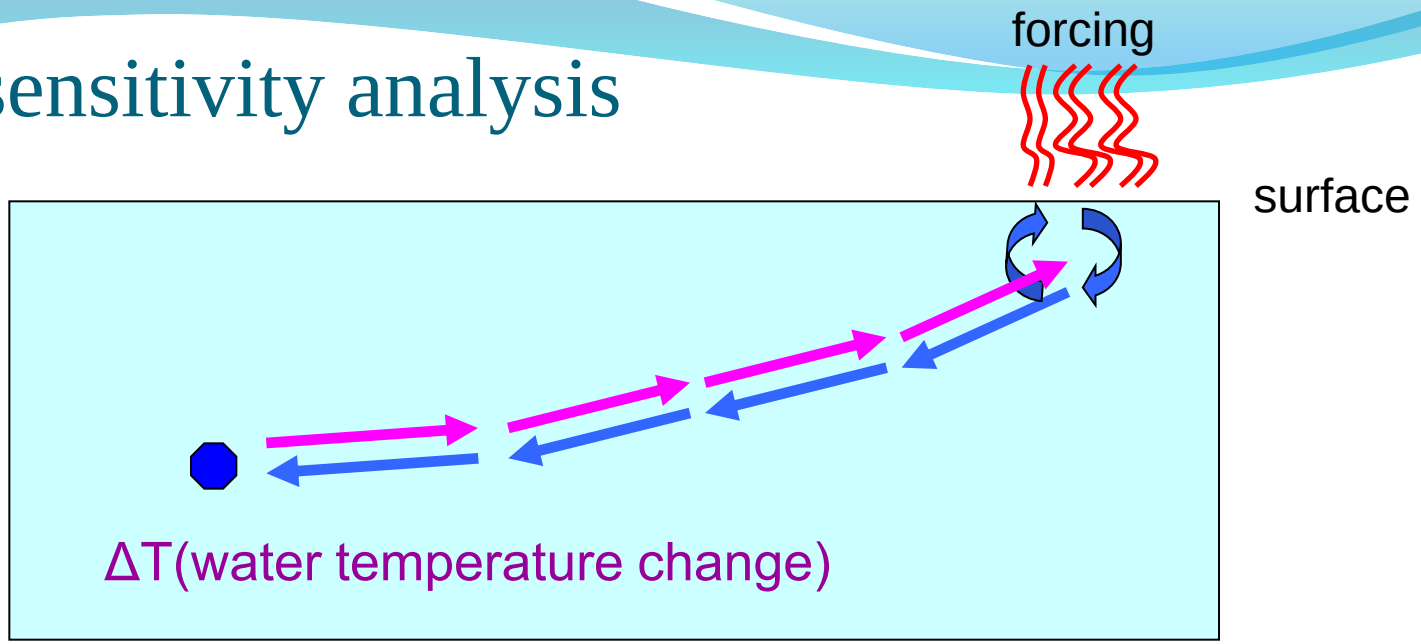

An adjoint sensitivity analysis moves the ocean representation backward in time.

The adjoint s f change of a physical vari variables (e.g., water tempe nsional continuum of one temporal and three spatial coordinates. This is equivalent to specifying the "sensitivity" of a variable to small perturbations in the parameters governing the oceanic state.

It is applied to identify the possible key regions involved in the deep ocean temperature changes.

Data Synthesis System (for an adjoint calculation)

Ocean data assimilation system has been constructed (K7 consortium: e.g., *Masuda et al., 2010*), based on a 4-dimensional variational (4D-VAR) adjoint approach, whose adjoint component can be used for an adjoint sensitivity analysis.

OGCM :

GFDL MOM3, quasi-global 75°S-80°N

horizontal res : 1°x1°, vertical res:45 levels

Spinup :

1. 3000-year with a climatological forcing (accelerated method)
2. 120-year as climatological seasonal march.
3. 10-year with interannual forcings from NCEP/DOE.

Use of optimal parameters :

Green's function method is applied to some physical parameters (Toyoda et al.,20XX).

Data sysnthesis :

method : strong constrain 4D-VAR adjoint.

adjoint coding: by TAMC with some modifications.

assimilation window : 55 years (1957-2011)

control variables : initial conditions, 10-daily surface fluxes

first guess : results from Spinup 3

assimilated elements : OISST,T,S （Ensembles ver.3 + Mirai RV near real-time data ）,AVISO SSH anomaly.

ESTOC (K7 ocean state estimation) as a background oceanic state

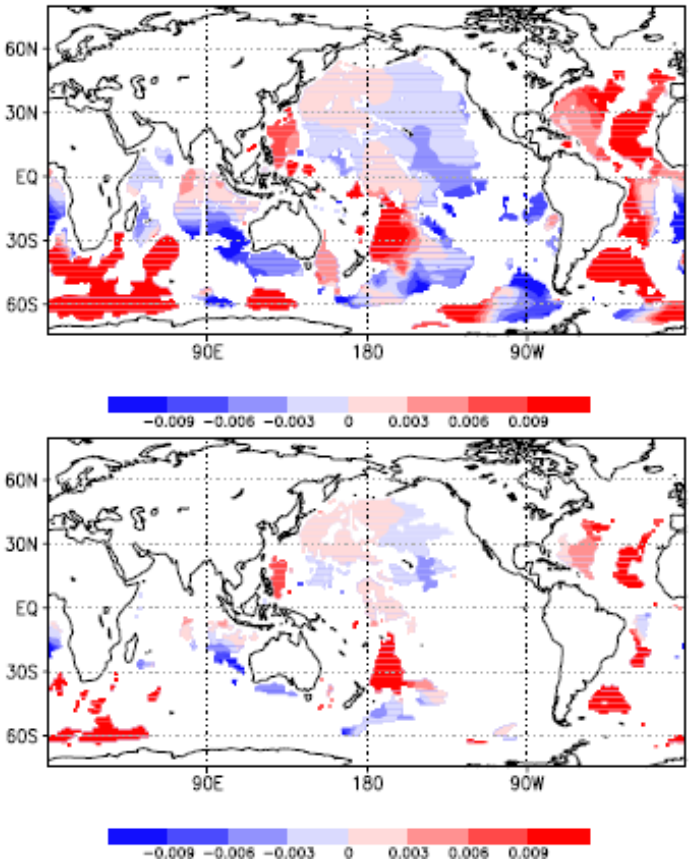

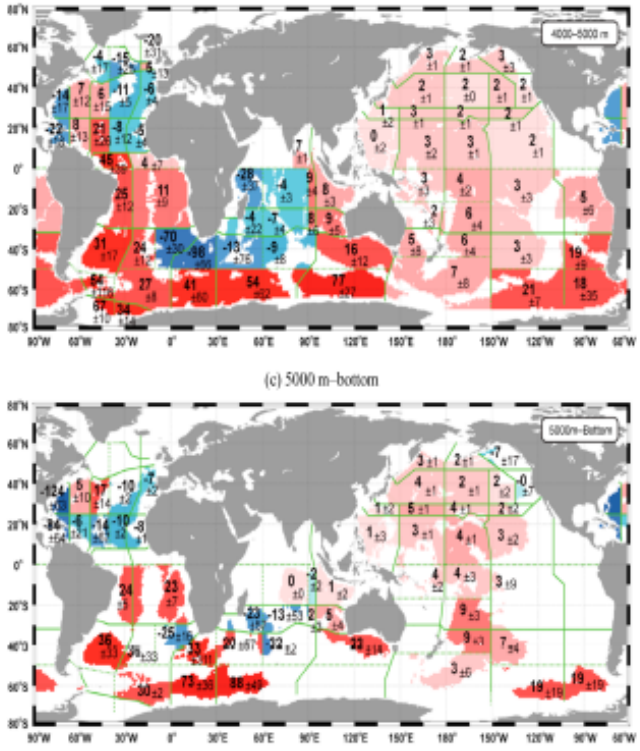

(Kouketsu et al., 2011)

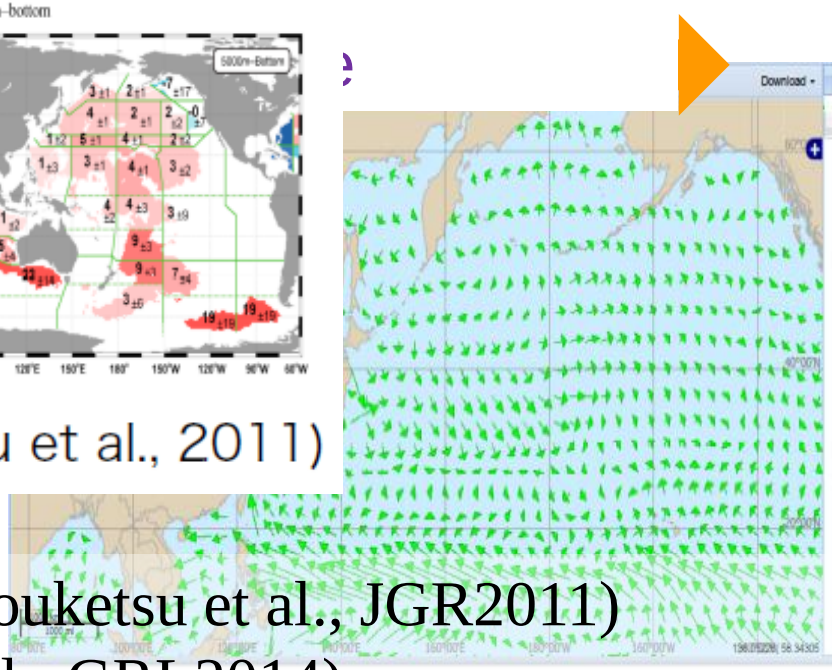

- HC change/Bottom-water warming (Kouketsu et al., JGR2011)
- 18.7yr climate resonance (Osafune et al., GRL2014)
- GOV/GSOP intercomparisons (e.g., Balmaseda et al., JOO2014)

Adjoint sensitivity analysis experiment

- Global heat content change (water temperature warming) below 2000m is our target. [Relevant artificial "cost" is given.]
- 20yr backward calculation on the "Earth Simulator".
- Adjoint variable for T been multiplied by the prior uncertainty estimate σ derived from the ESTOC and normalized by the cell volume

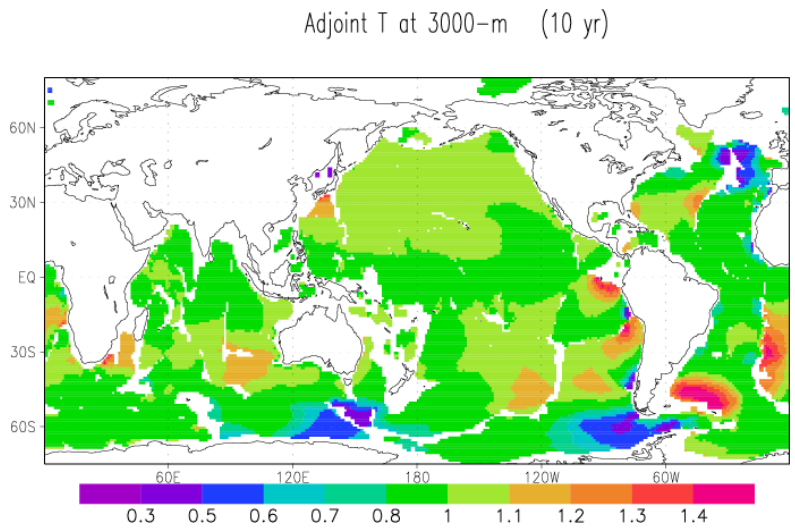

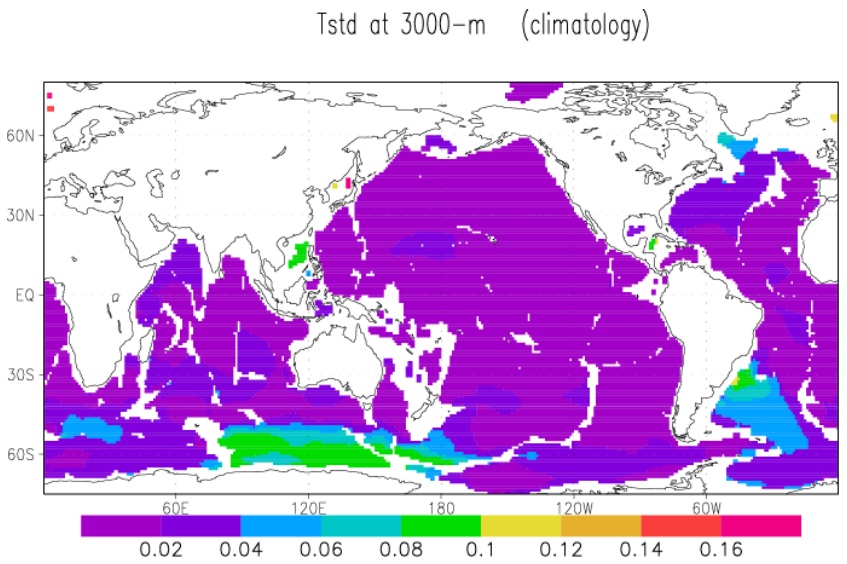

Appropriate "cost" for a trend signal

Sensitivity: $\nabla J[\delta_{t_2}] = \nabla J[(\delta_{t_2} + \delta_{t_1})/2] + \nabla J[(\delta_{t_2} - \delta_{t_1})/2].$

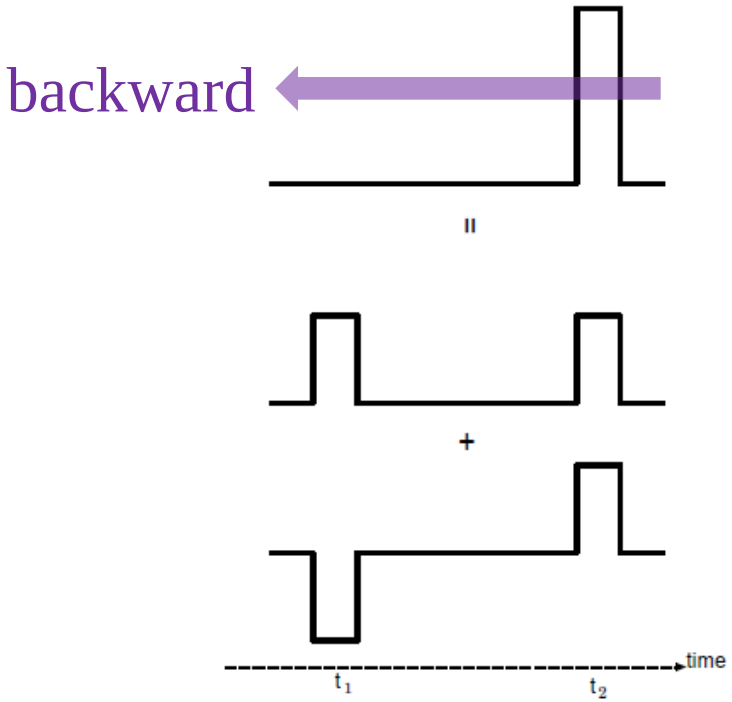

A warming signal at time t_2

Persistent warming signals influencing times t_1 & t_2

A set of warming trend signal from time t_1 to t_2

Here, we apply a set of warming trend signal to our sensitivity analysis as an artificial "cost". This can more clearly detect key sites for observation in conjunction with a bottom-water warming.

Sensitivity for Y2000 to a specific pentadal warming

Adjoint T at 3000−m depth * std (10 yr)

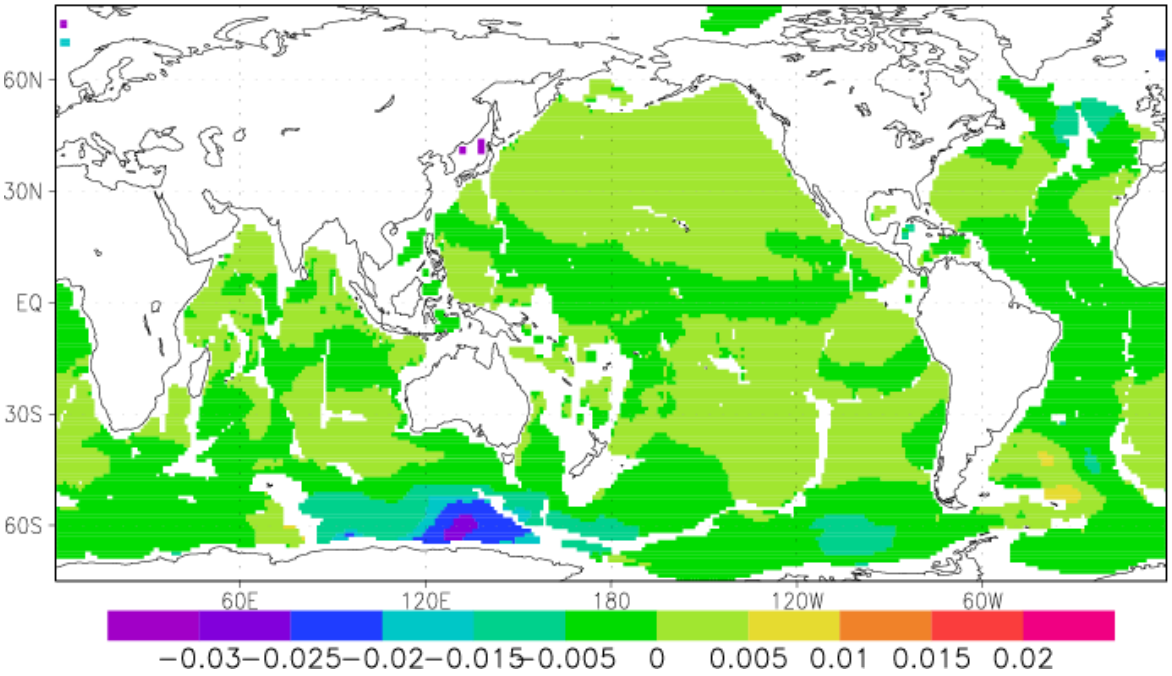

Sensitivity for Y1990 to a specific decadal warming

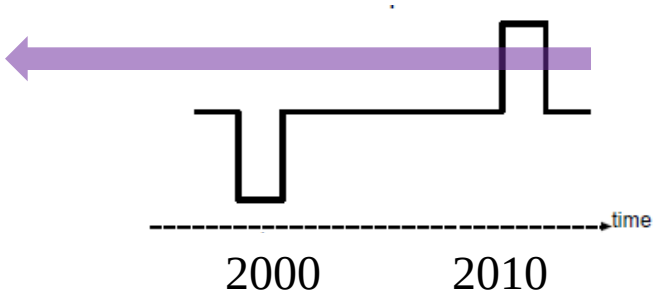

Adjoint T at 3000−m depth * std (20 yr)

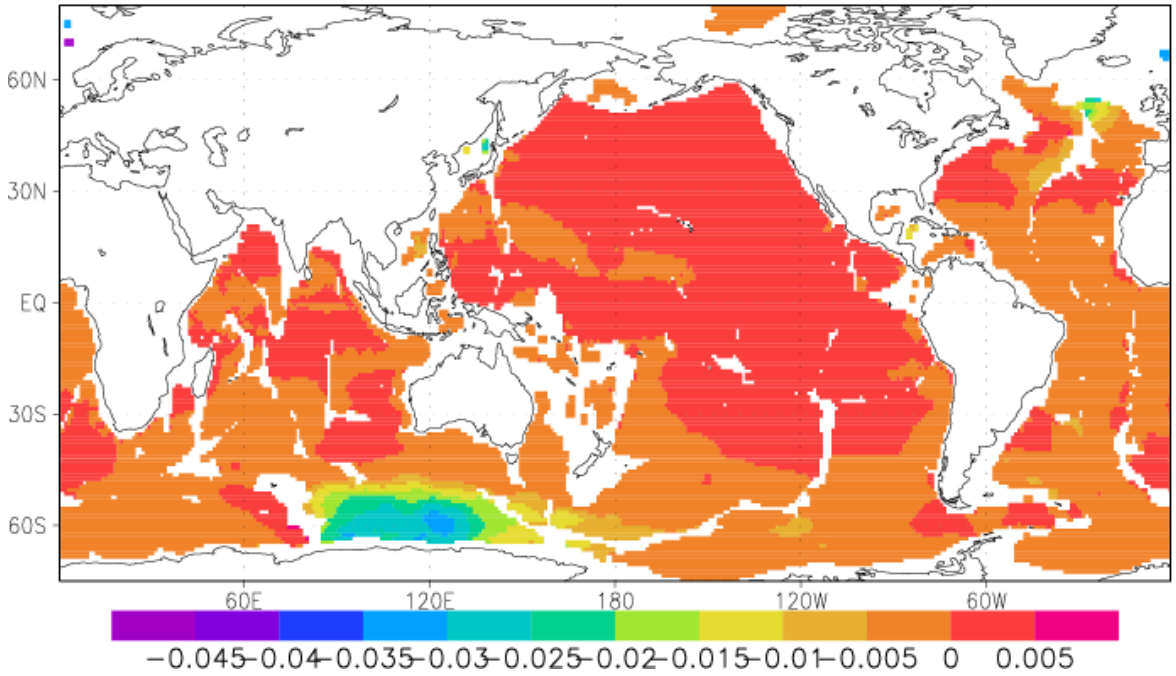

Sensitivity for Y2000 to a specific warming in 2010

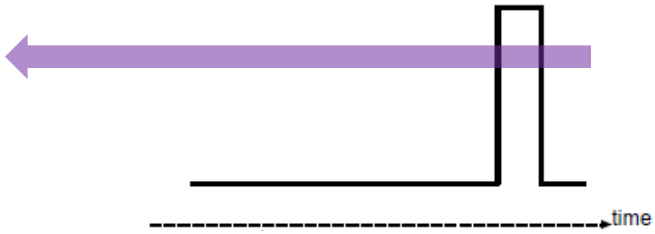

2010

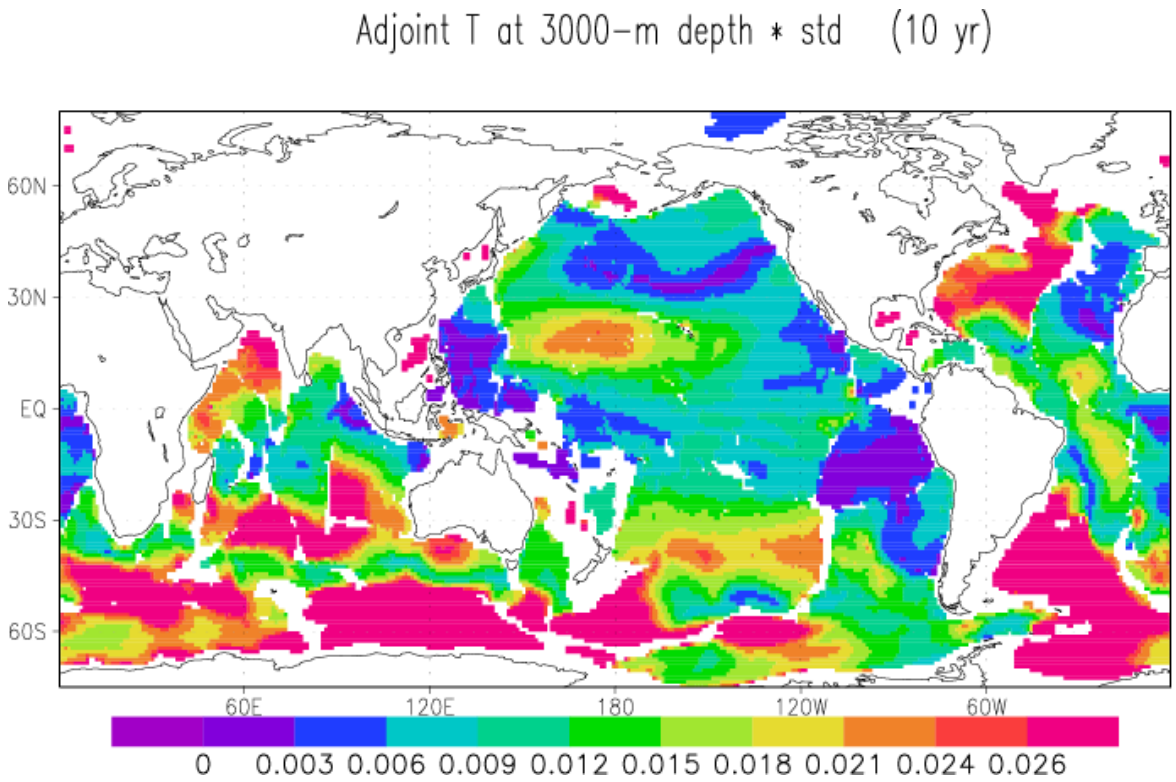

Corroborative observations for validation

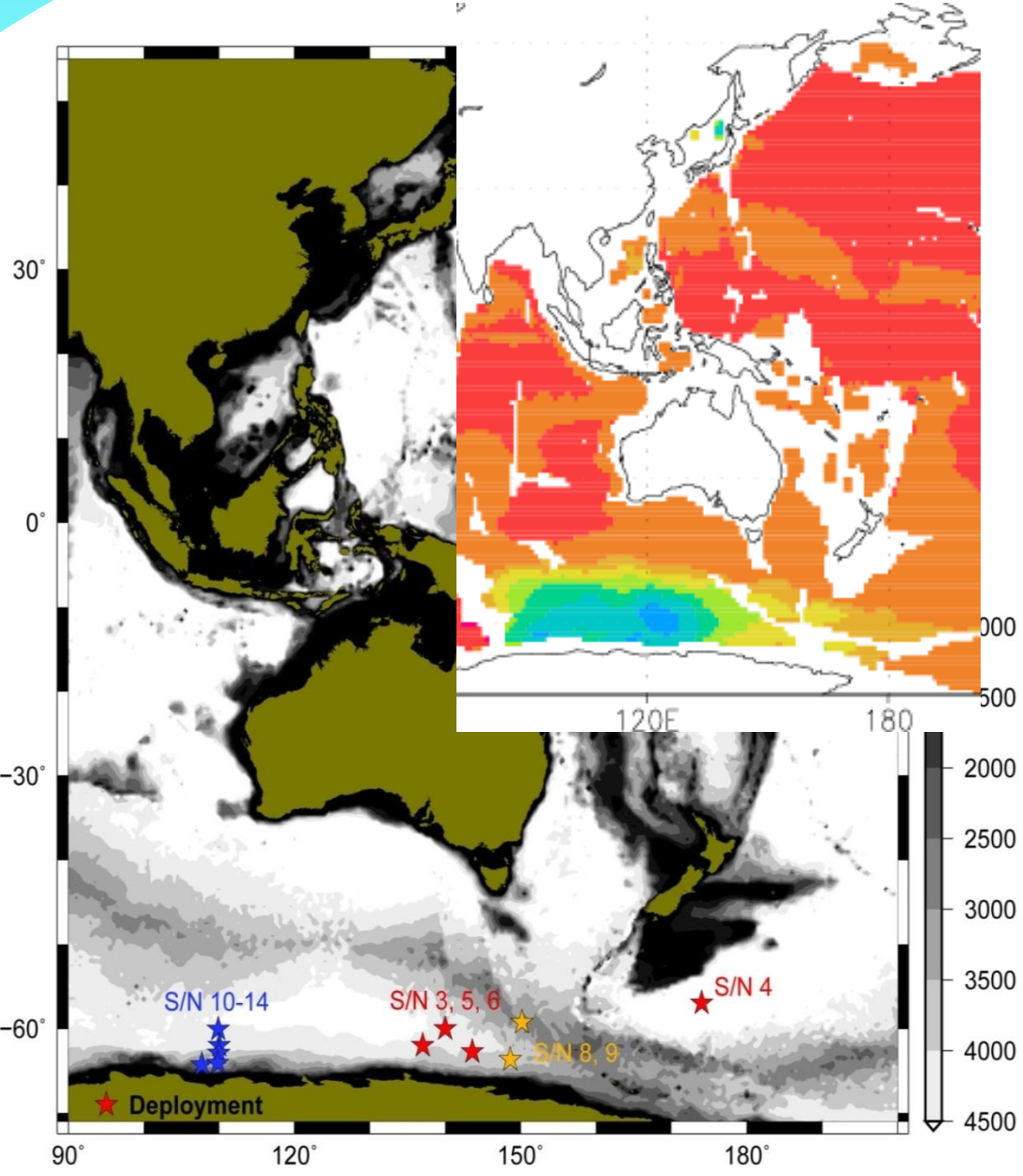

Deployment of Deep NINJA off the Adelie Coast, Antarctica, from R/V Mirai in December 2012.

We are deploying 11 Deep Ninjas in the key sites detected by the sensitivity exercise to make an improve state estimation and to uncover the mechanism of deep ocean changes.

Deep float data is now processing

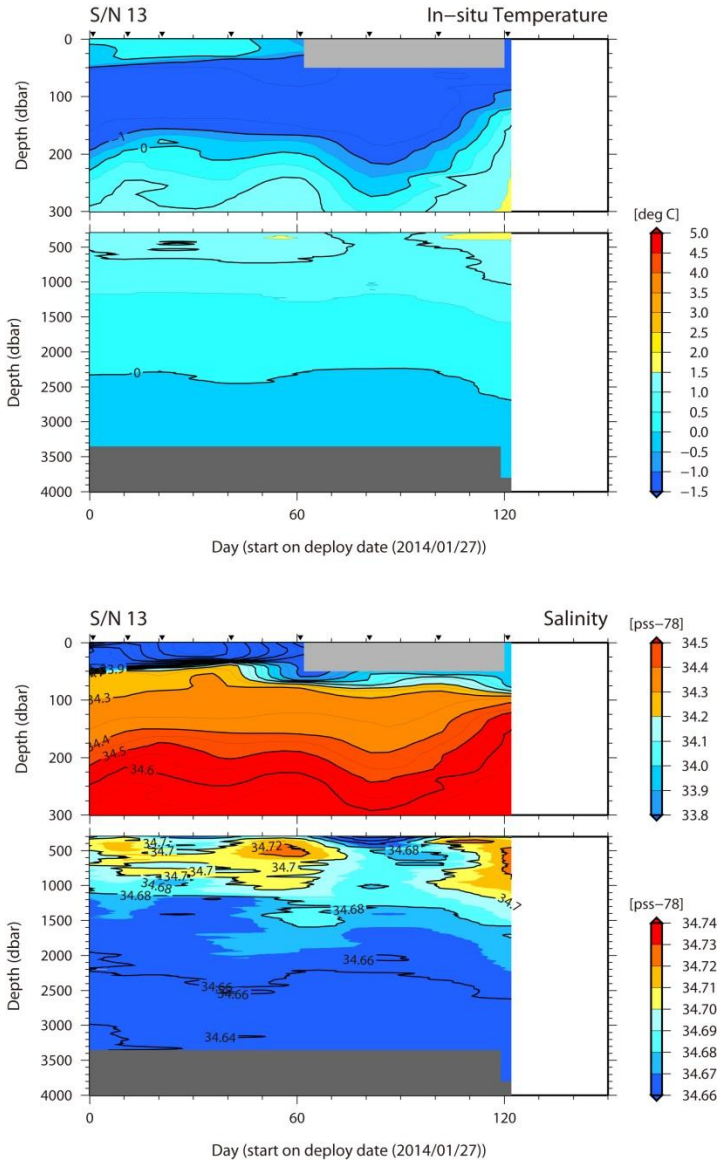

http://www.jamstec.go.jp/ARGO/deepninja/

Toward an Optimal Design of Deep Profiling Float Network:

OSE is planed by using two global data synthesis systems in JAMSTEC when making long-term state estimation;

1) The system used for sensitivity analysis (MOM3 base),

2) Another 4D-VAR system with finer resolution (tripolar MRI.COM base).

Since sensitivity may depend on the system, such a multi system analysis shall be preferable.

Summary toward an Optimal Design of Deep Profiling Float Network

An adjoint sensitivity analysis were applied to identify key regions for the bottom-water warming below 2000 m depth in the global ocean.

- *An adjoint sensitivity analysis implies that changes in the water temperature in the local areas in the Southern Ocean can have subtle influence on the water warming in the pentadal/decadal time-scale.*
- *We are deploying several Deep float around the key regions as corraborative observations.*
- *OSE by using multi data synthesis system with different architecture is planned, should be helpful to detect a general evaluation of the observing system.*

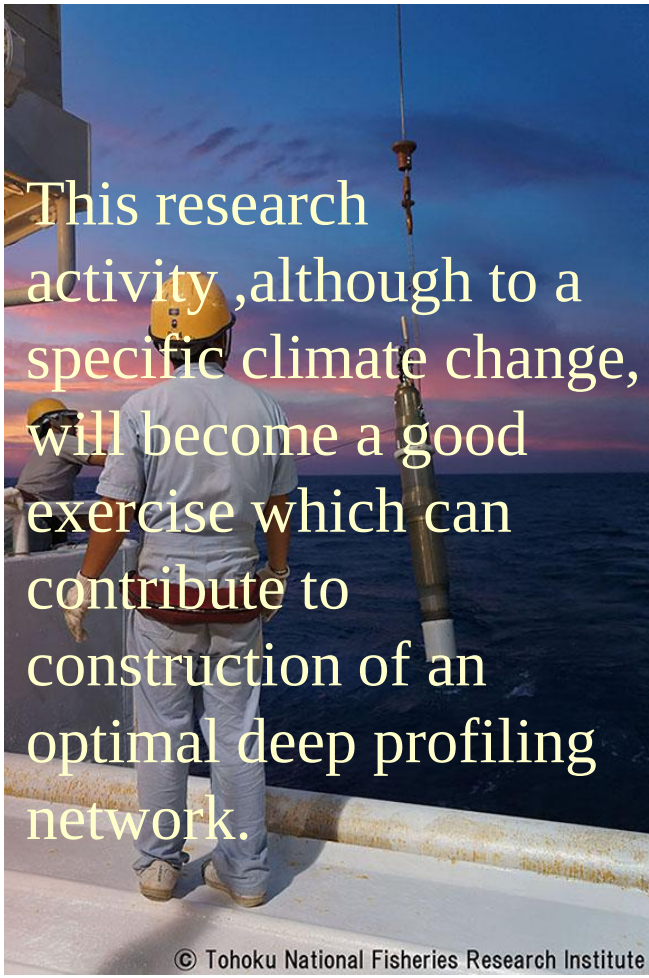

Fin

Cost function

$$J = \left[x - x_0\right]^T B_1^{-1}\left[x - x_0\right] + \left[H(x) - y^*\right]^T R^{-1}\left[H(x) - y^*\right]$$
$$+ \left[\nabla \cdot (x - x_0)\right]^T B_2^{-1}\left[\nabla \cdot (x - x_0)\right],$$

$here,\ y^* : observations$ (inc. model bias), x : control variable,

$H : observation\ matrix,$

$R : observation\ error$ (inc. representativeness error).

Assimilated elements: Temperature, Salinity (ENSEBLES v.3+JAMSTEC observations),
SST (reconstructed Reynolds+OISST ver.2),
SSH anomaly data (AVISO).

First guess is generated from
momentum, net heat, shortwave, latent heat flux of NCEP/DOE .

To uncover changes in deep waters

Deep NINJA has been developed since 2009 by JAMSTEC and Tsurumi Seiki Co. Ltd. (TSK)
Recently, the first prototype was assembled.
Results of the first test in coastal waters were good.

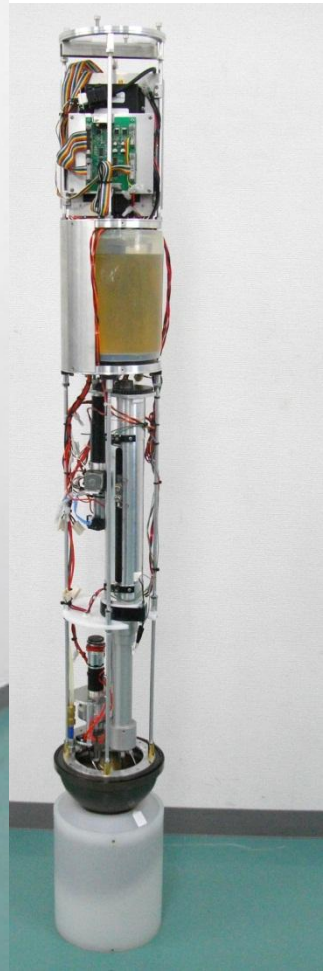

First prototype

Height: 210 cm (with antenna)

Weight: 50 kg (in air)

Max. depth: 4000 dbar for the global ocean

Sensor: SBE-CTD

Additional sensors are available in future.

Communication: Iridium (bi-directional)

Battery: Lithium

Lifetime (est.): 120 cycle

(Courtesy of Dr. Kobayashi)